Emildo Marcano*

DFT Study of Anthocyanidin and Anthocyanin Pigments for Dye Sensitized Solar Cells: Electron Injecting from the Excited States and Adsorption onto TiO_2 (Anatase) Surface

https://doi.org/10.1515/ehs-2018-0008

Abstract: We explored, the absorption spectra, excited states and electronic injection parameters of anthocyanidin and anthocyanin pigments using the level of theory (TD)CAM-B3LYP/6–31 + G(d,p). For all isolated dyes, the distribution pattern of HOMO and LUMO spread over the whole molecules, which lead an efficient electronic delocalization. The calculated LHEs are all near unity. Methoxy group in Peonidin molecule lead the largest oscillator strength and LHE. The presence of water lead a higher spontaneous electronic inject process, with ΔG_{inject} average of −1.14 eV. The ΔG_{inject} order is Peonidin < Delphinidin < Cyanin < Cyanidin. Similarly, the adsorption energies (E_{ads}) onto anatase surface model were obtained from level of theory GGA(PBE)/DNP. E_{ads} of anthocyanin-$(TiO_2)_{30}$ complex was calculated to be from 17 to 24 eV, indicating both, the strong interactions between the dyes and the anatase (TiO_2) surface and stronger electronic coupling strengths of the anthocyanin-$(TiO_2)_{30}$ complex, which corresponded to higher observed η. The HOMO and LUMO shape showed the electrons delocalized predominantly on the anthocyanin structure while, the LUMO + 1 shape is localized into the $(TiO_2)_{30}$ surface. Therefore we expected a electronic injection from HOMO to LUMO + 1 in the anthocyanin-$(TiO_2)_{30}$ adsorption complex, after the light absorption.

Keywords: anthocyanin, anatase (TiO_2) surface, adsorption energies, electronic injection

Introduction

Dye Sensitized Solar Cells (DSSC) based on organic dyes adsorbed on nanocrystalline TiO_2 electrodes have attracted considerable attention in recent years because of their high incident solar light → electricity conversion efficiency and low cost of production (Hagfeldt et al. 2010; Vittadini, Casarin, and Selloni 2007). The driving force in these is the interfacial electron injection from the dye to the semiconductor. Upon absorbing light, the dye molecules are excited from their ground state, which is located energetically in the semiconductor band gap, to an excited state that is resonant with the TiO_2 conduction band. The electron is then transferred to the semiconductor on the ultrafast time scale (Sánchez De Armas et al. 2010). The relative yields and rates of electron injection, recombination, and decay of the dye-excited state influence the efficiency of the solar cell (Xie et al. 2016). Therefore, improving the efficiency of the solar devices is possible only when the rates and mechanisms of the competing reactions are known and understood. This in turn requires knowledge of the electronic structure of the dyes both, before and after binding to the semiconductor surface (Duncan and Prezhdo 2005). The photochemical properties of different organic sensitizers have extensively been investigated in an attempt to design dyes with maximal visible light absorption coupled to long-lived excited states. However, major effort is still needed in both developing new sensitizers and finding optimal working conditions to improve the photon → current conversion efficiencies (Manzhos, Giorgi, and Yamashita 2015; Jungsuttiwong et al. 2012; Zhu, Liang, and Cao 2013). In this framework, natural dyes as photosensitizers for DSSCs are very attractive because they are of low cost, abundant in supply, and sustainable (Gao, Bard, and Kispert 2000; Hao et al. 2006; Monishka 2012; Hug et al. 2014). Specifically, several types of natural dyes belonging to Anthocyanin have been performed. The anthocyanins belong to the group of natural dyes responsible for several colors in red-blue range, found in fruits, flower and leaves of plants. The dyes extracted from grape, mulberry, blackberry, red Sicilian orange, Sicilian prickly pear, eggplant and radicchio have shown a monochromatic incident photon to current efficiency (IPCE) ranging from 40 % to 69 %. Short circuit photocurrent densities (J_{sc}) up to 8.8 mA/cm^2, open circuit voltage (V_{oc}) ranging from 316 to 419 mV and solar conversion efficiency of 2.06 % (Calogero et al. 2012; Alhamed, Issa, and Doubal 2012; Suhaimi et al. 2013). Despite several

***Corresponding author: Emildo Marcano,** Universidad Pedagógica Experimental Libertador, Instituto Pedagógico de Caracas, Centro de Investigaciones en Ciencias Naturales (CICNAT), Laboratorio de Química Computacional, Apartado, Caracas 1020-A, Venezuela, E-mail: jedi148@gmail.com

experimental results about the performance of Anthocyanin pigments in DSSC, there are no systematic calculations of their electron transference mechanism from the excited states and adsorption onto TiO_2 surface to the best of our knowledge. Within this framework, the main objectives of this paper is to explore, using theoretical calculations, the electronic properties of anthocyanidin and anthocyanin pigments after and before adsorption onto TiO_2 (anatase) surface. The characterization of electronic properties for dyes in gas phase were carried out using the level of theory CAM-B3LYP, employing the 6–31 + G(d,p) basis set. The absorption spectra, excited states and electronic injection parameters were obtained and analyzed at TD(CAM-B3LYP)/6–31 + G(d,p). Finally, the adsorption energies onto anatase surface model were obtained and analyzed at DFT level using GGA(PBE) functional and numerical DNP basis set.

Theory and Computational Details

The sunlight-to-electricity conversion efficiency (η) of solar cell devices is determined by open-circuit photovoltage (V_{OC}), short-circuit current density (J_{SC}) and the fill factor (FF), as compared to incident solar power (P_{inc}) (Hagfeldt et al. 2010; Feng et al. 2013; Zhang 2013):

$$\eta = FF\,\frac{V_{OC}\,J_{SC}}{P_{inc}} \tag{1}$$

J_{SC} is determined by the following equation:

$$J_{SC} = \int LHE(\lambda)\;\Phi_{inject}\;\eta_{collect}\;d\lambda \tag{2}$$

where, $\eta_{collect}$ is the charge collection efficiency, for the same DSSCs differing only in the dye, as is the case for the organic dyes under study, it is reasonable to assume that this parameter is constant. LHE (λ) (light harvesting efficiency) is the fraction of the incident photons that are absorbed by the dye. LHE is related to the oscillator strength (*f*) at a given wavelength. By the following equation, while the larger *f*, the stronger LHE (O'Regan and Gratzel 1991):

$$LHE = 1 - 10^{-f} \tag{3}$$

The Φ_{inject} parameter evinces the electron injection efficiency and is related to the driving force ΔG_{inject} of electrons injecting from the excited states of dye molecules to the semiconductor substrate. It can be estimated as (Abdullah et al. 2013):

$$\Delta G_{inject} = E_{OX}^{dye^*} - E_{CB}^{TiO_2} \tag{4}$$

$E_{OX}^{dye^*}$ is the excited state oxidation potential of the dye. $E_{CB}^{TiO_2}$ is the energy of conduction band of the TiO_2 semiconductor (–4 eV). $E_{OX}^{dye^*}$ can be determined using following formula:

$$E_{OX}^{dye^*} = E_{OX}^{dye} - \lambda_{max}^{ICT} \tag{5}$$

In equation (5) λ_{max}^{ICT} is the energy of intermolecular charge transfer (ICT).

Density functional theory (DFT) and time dependent density functional theory (TDDFT) calculations were performed to determine geometries, electronic structures and electronic absorption spectra of anthocyanin dyes. All the calculations, in gas phase, were performed using GAMESS package (Schmidt, Baldridge, and Boatz 1993). All calculations were performed by employing CAM-B3LYP/6–31 + G(d,p). On the basis of equations (3)-(5), we calculated LHE and ΔG_{inject} parameters and analyzed the efficiency of anthocyanin dyes for electron injection from dye's excited state to TiO_2 (anatase) surface (Martsinovich and Troisi 2011; Zhang et al. 2012).

The adsorption of dyes on the anatase cluster was performed with DFT calculations using DMol^3 program (Delley 2000). The model employed herein to represent the (100) surface of anatase consists of 30 TiO_2 units, terminated with 12 hydrogen atoms, which modeled a TiO_2 nanoparticle (Koch et al. 2011). The initial structure has been taken from the crystal of TiO_2 anatase (Greeves). This model has a diameter of about 1 nm, that has to be compared to nanoparticles of about 2–6 nm used in experiments, and has been used in theoretical study of electronic absorption spectrum of organic compound supported on TiO_2, with application in dye sensitized solar cells (Sánchez De Armas et al. 2010).

The $(TiO_2)_{30}$ configurations were fully optimized using the generalized gradient-corrected approximation (GGA). The Perdew–Burke–Ernzerhof (PBE) functional was used to account exchange–correlation effects with DNP basis set. The core electron was treated with DFT-semicore Pseudopotentials (DSPPs). After optimization, the adsorption energies (E_{ads}) on the $(TiO_2)_{30}$ cluster were obtained. The latter value was obtained using the equation:

$$E_{ads} = E_{TiO_2+Anth} - E_{TiO_2} - E_{Anth} \tag{6}$$

where E_{TiO_2+AmA} is the total energy of Anthocianin-$(TiO_2)_{30}$ complex, E_{TiO_2} is the energy for the anatase surface model and E_{Anth} is the energy for the anthocyanin molecule (Srinivas et al. 2011). Following the above expression, the negative value of E_{ads}, indicated a stable adsorption.

Results and Discussion

Geometric Optimization and Intramolecular Charge Transferences of Anthocyanin Dyes

The anthocyanin chromophores molecule (cyaniding, delphinidin, peonidin and cyanin) used to carry out the calculations are display in Figure (1)). They have a positive charge on the molecule, which enables it to absorb light and thus have color (Calogero et al. 2012). As observed in Figure (1)), Cyanidin and Delphinidin differ in the number of hydroxyl groups present in the molecule, while, Peonidin have a substituted –OH group. Cyanin have a glucoside group. From level of theory CAM-B3LYP/6–31 + G(d,p) all structures showed a planar geometric, which facilitates the electronic delocalization in all the structure. The glucoside group in Cyanine dye led a small deviation in the torsion angle for the [C3-C2-C1´- C2´] bond (14°).

Frontier Molecular Orbitals, Absorption Spectra and LHE

The ground state first singlet excited state excitation process can be mainly assigned to the HOMO–LUMO transition, which correspond to a π-π* excited singlet state. For the sake of characterizing electronic properties, it is useful to examine the distribution patterns of molecular orbitals (Chang and Chow 2009), (Kulhánek and Bureš 2012). On the other hand, an important thermodynamic requirement of the dyes to be used in DSSC technology is that the HOMO level of the sensitizer has to be sufficiently positive in the redox potential for efficient regeneration of the oxidized dye molecule to its original state by the iodide electrolyte and the LUMO energy of the dye has to be sufficiently higher than the conduction band edge of the semiconductor (E_{CB}). To demonstrate their characteristic electronic structure, the HOMO-LUMO shape from the anthocyanin molecules at CAM-B3LYP/6–31 + G(d,p) methods in gas phase, are shown in Figure (2)), and the energy parameter, including solvent (water) effects with IEFPCM model, are shown in

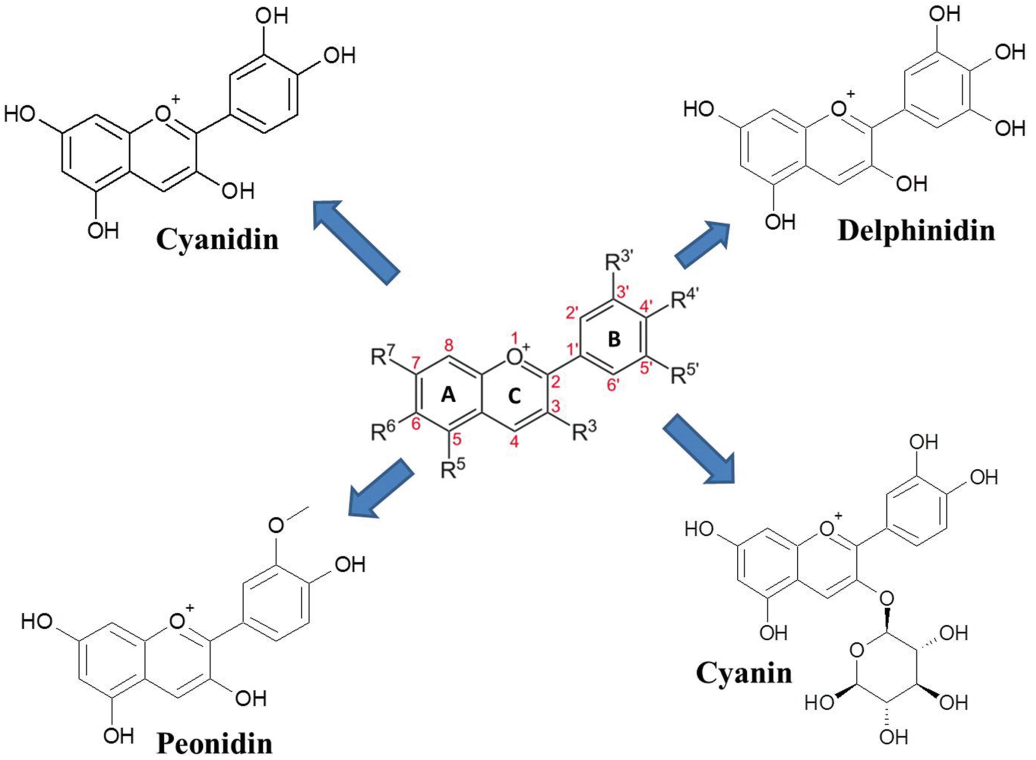

Figure 1: Anthocyanin chromophores molecules (cyaniding, delphinidin, peonidin and cyanin) studied in this work.

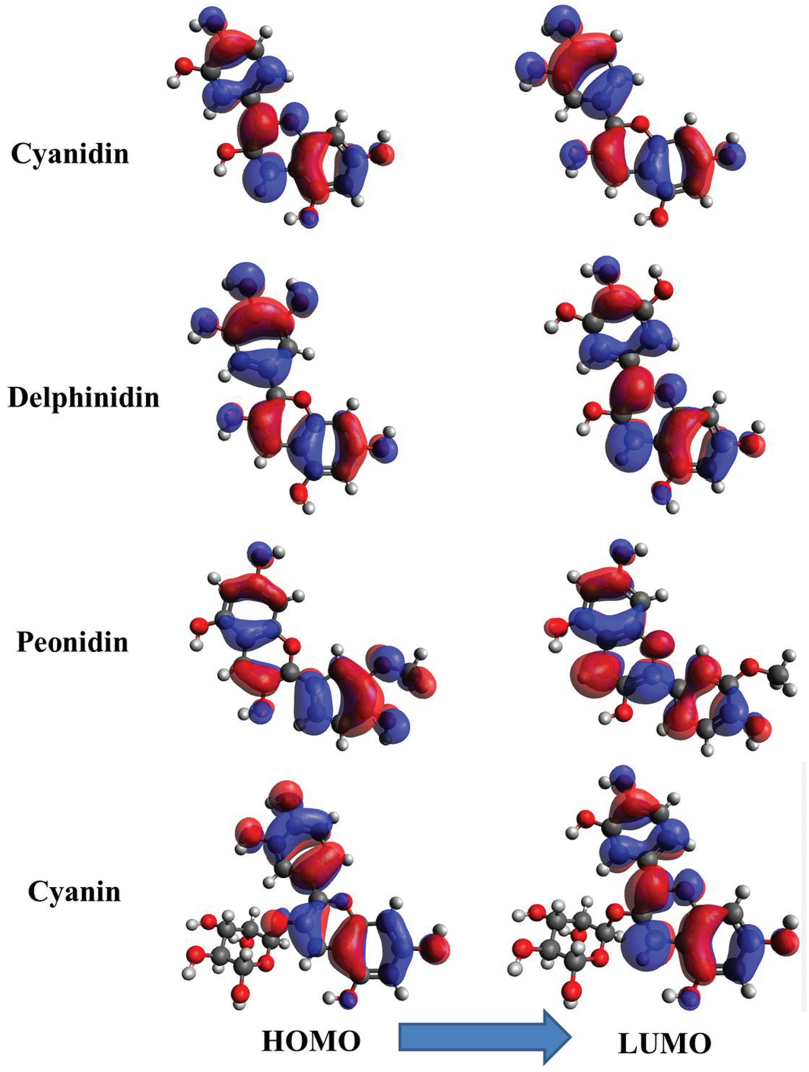

Figure 2: HOMO-LUMO shape from the anthocyanin molecules at CAM-B3LYP/6–31 + G(d,p) theory level in gas phase.

Table 1. With exception of Cianin, the distribution pattern of HOMO and LUMO spread over the whole molecule, as expected, in both, gas phase and water, which lead an efficient electronic delocalization (Calogero et al. 2012). In fact, the electronic density is shifted from the catechol moiety in ring B to the benzopyran system (ring A and C) (see Figure (1)). Independently of the substituted groups, in gas phase, the energy values for the HOMO and LUMO orbitals are close to the average −10.46 eV and −5.65 eV, respectively, in agreement with others reports (El Kouari et al. 2015), which underestimate the value corresponding to the conduction band of the anatase (−4 eV). When the effects of solvent are account, these values are increased up to −7 eV < −4 eV < −2 eV range (Eka et al. 2015). Therefore, the LUMO energy is sufficiently higher than the conduction band edge of TiO_2, and HOMO level is lower than the redox potential of I^-/I_3^- electrolyte to regenerate the oxidized dye (−4,6 eV) (Duncan and Oleg 2007; Zhang et al. 2009).

The calculations of the wavelength of maximum absorption (λ_{max}) and others spectroscopic parameter in water are shown in Table 2 at TD(CAM-B3LYP)/6–31 + G (d,p). Absorption spectra for anthocyanin molecules in gas phase and water are shown in Figure (3)). The prediction of absorption spectra for structures studied lead two maximum wavelength in 200 nm-250 nm range, and 400 nm-450 nm range, as expected (Eka et al. 2015; Zhang et al. 2009; Soto-Rojo et al. 2014). The λ_{max} values associated with the intramolecular charge transference (ICT), and HOMO → LUMO transition, is in the order Cyanidin (446 nm) > Peonidin (445 nm) > Delphinidin (442 nm) > Cyanin (438 nm). From Delphinidin molecule, the lack of a hydroxyl group lead a two extra maximum

Table 1: Computed HOMO, LUMO and energy gap (eV) in the gas phase and water at CAM-B3LYP/6–31 + G(d,p) level.

	Gas phase			Water		
Molecule	E_{HOMO}	E_{LUMO}	E_{gap}	E_{HOMO}	E_{LUMO}	E_{gap}
Cyanidin	−10.5803	−5.7686	4.8117	−5.6660	−2.6172	5.0489
Delphinidin	−10.4320	−5.6154	4.8166	−5.6405	−2.5796	5.0608
Peonidin	−10.3659	−5.6734	4.6925	−5.6008	−2.6107	4.9901
Cyanin	−10.4992	−5.5578	4.9414	−5.7030	−2.5908	5.1122
Average	−10.4693	−5.6538	4.8156	−5.6526	−2.5996	5.0530

Table 2: Wavelength of maximal absorption (λ_{max}/nm), excitation energies (E_e/eV, in water, TD(CAM-B3LYP)/6–31 + G(d) level), electronic transition configurations (Assignment), oscillator strengths (*f*) (*f* > 0.1) and LHE for anthocyanin dyes.

Molecule	λ_{max}	**Assignment**	**Ee**	***f***	**LHE**
	446.2	HOMO → LUMO (0.68)	2.78	0.742	0.8187
Cyanidin	229.2	HOMO-4 → LUMO (0.56)	5.41	0.244	
	205.6	HOMO → LUMO + 2 (0.49)	6.03	0.283	
	442.2	HOMO → LUMO (0.67)	2.80	0.744	0.8198
Delphinidin	228.4	HOMO-2 → LUMO + 1 (0.37)	5.43	0.321	
	206.2	HOMO → LUMO + 3 (0.46)	6.01	0.322	
	445.7	HOMO → LUMO (0.66)	2.78	0.767	0.8290
Peonidin	228.4	HOMO-2 → LUMO + 1 (0.36)	5.43	0.309	
	207.1	HOMO → LUMO + 2 (0.36)	5.99	0.437	
	438.7	HOMO → LUMO (0.68)	2.83	0.723	0.8107
Cyanin	250.8	HOMO → LUMO + 1 (0.63)	4.94	0.264	
	237.6	HOMO-1 → LUMO + 1 (0.37)	5.22	0.264	

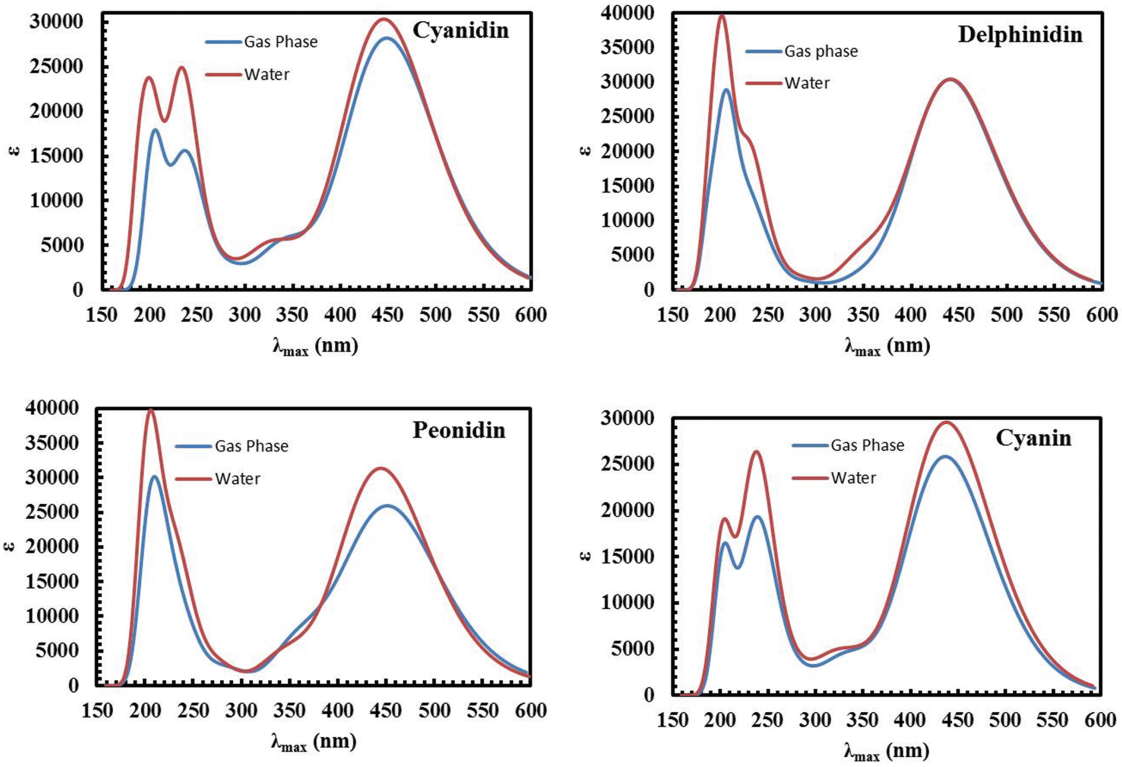

Figure 3: Absorption spectra for anthocyanin molecules in gas phase and water at TD(CAM-B3LYP)/6–31 + G(d,p) theory level.

wavelength, associated with the transitions HOMO-4 → LUMO (229 nm) and HOMO → LUMO + 2 (205 nm). Similarly, the substitution of a glucoside group in Cyanin structure, lead a two extra maximum wavelength, associated with the transitions HOMO → LUMO + 1 (250 nm) and HOMO-1 → LUMO + 1 (237 nm).

According the equations (1) and (2), LHE is one of the key factors in DSSC. It represents the fraction of the incident photons that are absorbed by the dye. The LHE of the dye should be as high as feasible to maximize the photo-current response. As observed in Table 2, the calculated LHEs are all near unity. Methoxy group in Peonidin molecule lead the largest oscillator strength and LHE. On the other hand, from Delphinidin molecule, the lacks of a hydroxyl group lead a decreased in the LHE. Similarly, when a glucoside group is substituted in Cyanin structure, a decreased in the LHE vale is found.

Free Energy Change of Electron Injection

On the basis of the knowledge of isolated dyes, we extend to study the driving force ΔG_{inject} of electrons injecting from the excited states of anthocyanin dye to the TiO_2 semiconductor substrate to analyze other factors affecting the energy conversion efficiency. Therefore, we have used eqs. (4) and (5) to estimate the anthocyanin's excited state oxidation potential and free energy change of electron injection to titanium dioxide TiO_2 surface, in gas phase and water from level of theory TD(CAM-B3LYP)/6–31 + G(d,p). E_{OX}^{dye} had been estimated as negative E_{HOMO} (Preat et al. 2009). The results are shows in Table 3. The solvent effects were evidenced in the E_{HOMO} results, which lead a significant decreased in ΔG_{inject}. Therefore, in gas phase, ΔG_{inject} have an average of 3.66 eV, while, the water presence lead a higher spontaneous electronic inject process, with ΔG_{inject} average of –1.14 eV. The negative ΔG_{inject} is an indication of spontaneous electron injection from the dye to TiO_2. For the anthocyanin molecules studied, the ΔG_{inject} order is Peonidin < Delphinidin < Cyanin < Cyanidin.

Chemisorption on TiO_2-anatase

Tetragonal structure of anatase may be described using two cell edge parameters, a and c, and one internal parameter, d (the length of the Ti–O apical bond) (Preat et al. 2009). In this paper, the $(TiO_2)_{30}$ configurations were optimized using the generalized gradient-corrected approximation (GGA). The results for the geometric parameters described before were a = 3.566 Å, c = 10.707 Å and d = 1.899 Å, which were comparable with experimental values (a = 3.782 Å, c = 9.502 Å, d = 1.979 Å) and others theoretical DFT methodology, where cluster approach methodology had been used (Preat et al. 2009; Bourikas, Kordulis, and Lycourghiotis 2014; Burdett et al. 1987).

In dye-TiO_2 adsorption, the adsorption of dyes through terminal –H atom can be either physisorption (via hydrogen bonding between an oxygen atom on TiO_2 surface and a hydrogen atom of the dye) or chemisorption (an H atom dissociates and the bond is formed between oxygen atoms and the surface titanium atoms of TiO_2. In this paper, we have chosen the second option. The adsorption complex was first fully optimized using the PBE functional together with the Double-Numerical with polarization performed in the DMol^3 program. The optimized structures of anthocyanin-$(TiO_2)_{30}$ adsorption complexes are show in Figure (4)) and the important optimized bond length and adsorption energy (E_{ads}) are listed in Table 4. The bond distances between Ti and O atom of dyes were calculated to be in the range of 1.89–1.97 Å. The adsorption energy (E_{ads}) of anthocyanin-$(TiO_2)_{30}$ complex was calculated to be from 17 to 24 eV, indicating the strong interactions between the dyes and the anatase (TiO_2) surface. The Table 4 shows that a systematic change in the sunlight-to-electricity conversion efficiency (η) was observed as predicted from adsorption energies. Therefore, the higher adsorption energy resulted in the stronger electronic coupling strengths of the anthocyanin-$(TiO_2)_{30}$ complex, which corresponded to higher observed η as expected (Henwood and David 2008).

In order to explore the possible intramolecular charge transference between anthocyanin dyes and anatase surface, HOMO and LUMO shape were examined by the DFT (PBE) calculations with DNP basis set. Numerical basis set were used because of its reasonable computational cost. Figure (5)) shows the frontier molecular orbitals of anthocyanin-$(TiO_2)_{30}$ adsorption complex in vacuum. The HOMO and LUMO shape showed the electrons delocalized predominantly on the anthocyanin structure while, the LUMO + 1 shape is localized into the $(TiO_2)_{30}$ surface. Therefore we expected an electronic injection from HOMO to LUMO + 1 in the anthocyanin-$(TiO_2)_{30}$ adsorption complex, after the light absorption.

Table 3: Anthocyanin's excited state oxidation potential and free energy change of electron injection to titanium dioxide TiO_2 surface, in gas phase and water at TD(CAM-B3LYP)/6–31 + G(d,p) theory level.

	Gas phase				Water			
Molecule	E^{dye}_{ox}	λ^{ICT}_{max}	E^{dye*}_{ox}	ΔG_{inject}	E^{dye}_{ox}	λ^{ICT}_{max}	E^{dye*}_{ox}	ΔG_{inject}
Cyanidin	10.4320	2.7579	7.6741	3.6741	5.6660	2.7784	2.8876	−1.1124
Delphinidin	10.3659	2.8091	7.5568	3.5568	5.6405	2.8036	2.8369	−1.1631
Peonidin	10.4992	2.7204	7.7788	3.7788	5.6008	2.7820	2.8188	−1.1812
Cyanin	10.4693	2.8316	7.6377	3.6377	5.7030	2.8261	2.8769	−1.1231
Average	10.4416	2.7798	7.6619	3.6619	5.6526	2.7975	2.8551	−1.1449

Table 4: Important optimized bond length Ti-O (Å), adsorption energy (E_{ads}/eV) and sunlight-to-electricity conversion efficiency, η(%) for anthocyanin-$(TiO_2)_{30}$ adsorption complexes.

Molecule	Ti-O	E_{ads}	η (%)
Cyanidin	1.93	17.624	0.37
Delphinidin	1.97	18.749	0.56
Peonidin	1.89	17.889	0.62
Cyanin	1.95	24.107	0.66

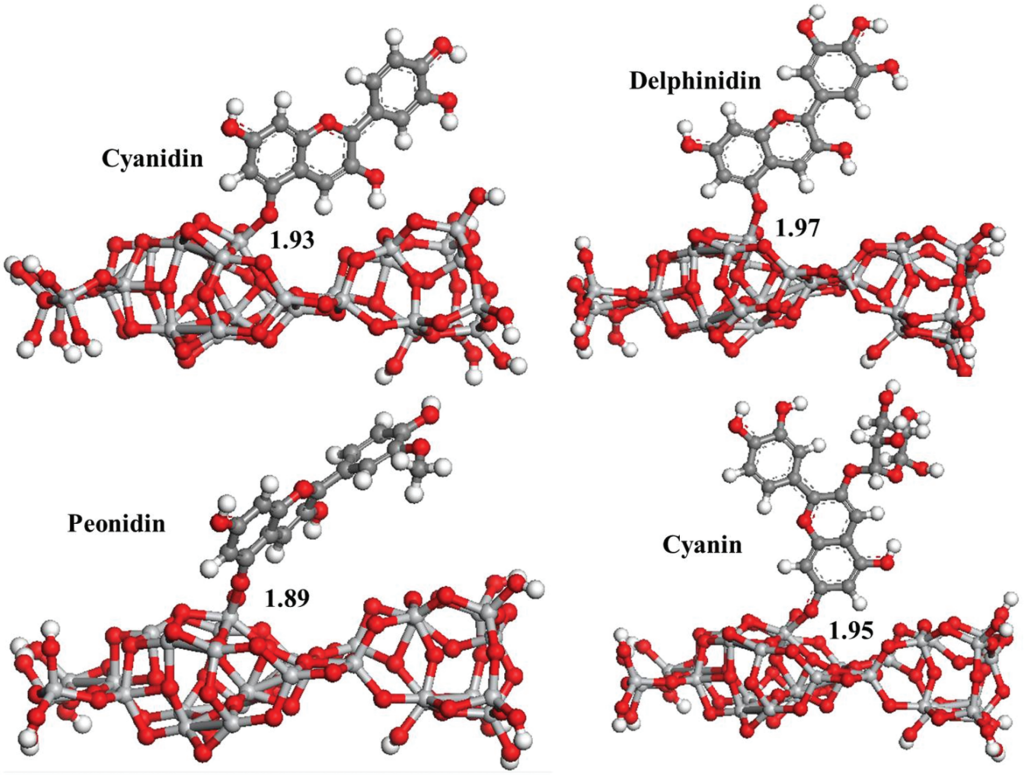

Figure 4: Optimized structures of anthocyanin-$(TiO_2)_{30}$ adsorption complexes at PBE/DNP theory level. Important optimized bond length are show in Å.

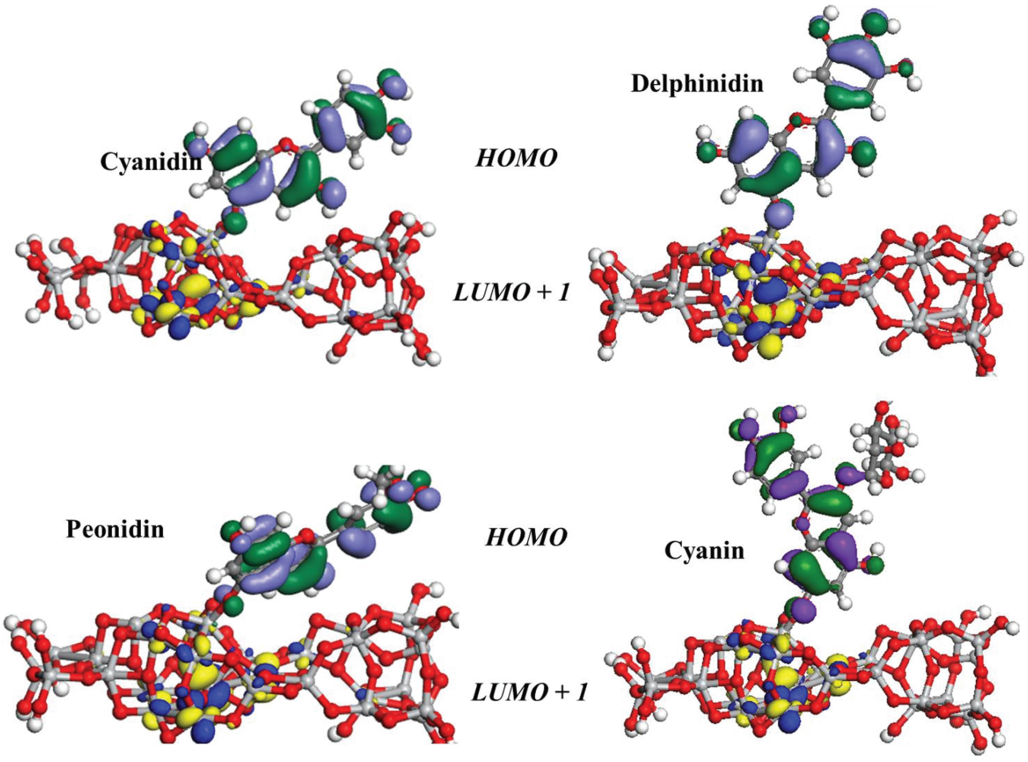

Figure 5: The HOMO (blue/green) and LUMO + 1 (blue/yellow) shapes of anthocyanin-$(TiO_2)_{30}$ adsorption complexes at PBE/DNP theory level.

Conclusions

We explored, the electronic properties of anthocyanidin and anthocyanin pigments after and before adsorption onto TiO_2 (anatase) surface. The characterization of electronic properties for dyes in gas phase and water were carried out using CAM-B3LYP/6–31 + G(d,p) methods. The absorption spectra, excited states and electronic injection parameters were obtained and analyzed at TD (CAM-B3LYP)/6–31 + G(d,p). The adsorption energies onto anatase surface model were obtained and analyzed at DFT level using GGA(PBE) functional and numerical DNP basis set. For all isolated dyes, the distribution pattern of HOMO and LUMO spread over the whole molecule, as expected, in both, gas phase and water, which lead an efficient electronic delocalization. The LUMO energy is sufficiently higher than the conduction band edge of TiO_2, and HOMO level is lower than the redox potential of I^-/I_3^- electrolyte to regenerate the oxidized dye. The calculated LHEs are all near unity. Methoxy group in Peonidin molecule lead the largest oscillator strength and LHE. The water presence lead a higher spontaneous electronic inject process, with ΔG_{inject} average of –1.14 eV. The negative ΔG_{inject} is an indication of spontaneous electron injection from the dye to TiO_2. For the anthocyanin molecules studied, the ΔG_{inject} order is Peonidin < Delphinidin < Cyanin < Cyanidin. The adsorption energy (E_{ads}) of anthocyanin-$(TiO_2)_{30}$ complex was calculated to be from 17 to 24 kcal/mol, indicating the strong interactions between the dyes and the anatase (TiO_2) surface. Therefore, the higher adsorption energy resulted in the stronger electronic coupling strengths of the anthocyanin-$(TiO_2)_{30}$ complex, which corresponded to higher observed η as expected. The HOMO and LUMO shape showed the electrons delocalized predominantly on the anthocyanin structure while, the LUMO + 1 shape is localized into the $(TiO_2)_{30}$ surface. Therefore we expected an electronic injection from HOMO to LUMO + 1 in the anthocyanin-$(TiO_2)_{30}$ adsorption complex, after the light absorption.

Acknowledgements: We acknowledge support by Fondo Nacional de Ciencia, Tecnología e Innovación (FONACIT) through grant PEI-1852.

References

Abdullah, Muhammad Imran, Muhammad Ramzan Janjua, Saeed Ashraf, Asif Mahmood, Sajid Ali, and Muhammad Ali. 2013.

"Quantum Chemical Designing of Efficient Sensitizers for Dye Sensitized Solar Cells. Bull." *Korean Chemical Social* 34: 2093–98.

Alhamed, Mounir, Ahmad S Issa, and Wael A Doubal. 2012. "Studying of Natural Dyes Properties as Photo-Sensitizer for Dye Sensitized Solar Cells (DSSC)." *Journal of Electron Devices* 16: 1370–83.

Bourikas, Kyriakos, Christos Kordulis, and Alexis Lycourghiotis. 2014. "Titanium Dioxide (Anatase and Rutile): Surface Chemistry, Liquid-Solid Interface Chemistry, and Scientific Synthesis of Supported Catalysts." *Chemical Reviews* 114: 9754–823.

Burdett, K, T Hughbanks, G. J. Miller, J. W Richardson, and J. V Smith. 1987. "Structural-Electronic Relationships in Inorganic Solids: Powder Neutron Diffraction Studies of the Rutile and Anatase Polymorphs of Titanium Dioxide at 15 and 295 K." *Journal American Chemical Social* 109: 3639–46.

Calogero, Giuseppe, Jun-Ho Yum, Alessandro Sinopoli, Di Marco Gaetano;, and Michael Gratzel. 2012. "Anthocyanins and Betalains as Light-Harvesting Pigments for Dye-Sensitized Solar Cells." *Solar Energy* 86: 1563–75.

Chang, Y. J, and T J. Chow. 2009. "Dye-Sensitized Solar Cell Utilizing Organic Dyes Containing Triarylene Conjugates." *Tetrahedron* 65: 4726.

Delley, B. 2000. "From Molecules to Solids with the DMol^3 Approach." *Journal Chemical Physical* 113: 7756.

Duncan, R Walter, and V Prezhdo Oleg. 2007. "Theoretical Studies of Photoinduced Electron Transfer in Dye-Sensitized TiO2." *Annual Reviews Physical Chemical* 58: 84–143.

Duncan, Walter R, and Oleg V Prezhdo. 2005. "Electronic Structure and Spectra of Catechol and Alizarin in the Gas Phase and Attached to Titanium." *Journal Physical Chemical B* 109: 365–73.

Eka, Cahya Prima, Brian Yuliarto, Hermawan Kresno Dipojono, and Suyatman Dipojono. 2015. "Theoretical Investigation of Anthocyanidin Aglycones as Photosensitizers for Dye-Sensitized TiO2 Solar Cells." *Advanced Materials Research* 1112: 317–20.

El Kouari, Y, A. Migalska-Zalas, A. K. Arof, and B. Sahraoui. 2015. "Computations of Absorption Spectra and Nonlinear Optical Properties of Molecules Based on Anthocyanidin Structure." *Optical Quant Electronic* 47: 1091–99.

Feng, Jie, Yang Jiao, Ma Wei, Md K Nazeeruddin, Michael GräTzel, and Sheng Meng. 2013. "First Principles Design of Dye Molecules with Ullazine Donor for Dye Sensitized Solar Cells." *Journal Physical Chemical C* 117: 3772–78.

Gao, Frank G, Allen J Bard, and Lowell D Kispert. 2000. "Photocurrent Generated on a Carotenoid-Sensitized TiO2 Nanocrystalline Mesoporous Electrode." *Journal of Photochemistry and Photobiology A: Chemistry* 130: 49–56.

Greeves, Nick. ChemTube3D. [on line] http://www.chemtube3d.com/index.html.

Hagfeldt, Anders, Gerrit Boschloo, Licheng Sun, Lars Kloo, and Henrik Pettersson. 2010. "Dye-Sensitized Solar Cells." *Chemical Reviews* 110: 6595–663.

Hao, Sancun, Wu Jihuai, Yunfang Huang, and Jianming Lin. 2006. "Natural Dyes as Photosensitizers for Dye-Sensitized Solar Cell." *Solar Energy* 80: 209–14.

Henwood, Daniel, and Carey, J. David. 2008. "Molecular Physisorption on Graphene and Carbon Nanotubes: A Comparative Ab Initio Study." *Molecular Simulation* 34: 1019–23.

Hug, Hubert, Michael Bader, Peter Mair, and Thilo Glatzel. 2014. "Biophotovoltaics: Natural Pigments in Dye-Sensitized Solar Cells." *Applied Energy* 115: 216–25.

Jungsuttiwong, S, R Tarsang, Y Surakhot, J Khunchalee, T Sudyoadsuk, V Promarak, and S. Namuangruk. 2012. "Theoretical Study of α-fluorenyl Oligothiophenes as Color Tunable Emissive Materials for Highly Efficient Electroluminescent Device." *Organic Electronics* 13: 1836–43.

Koch, Rainer, Andrew S Lipton, Filipek Slawomir, and Venkatesan Renugopalakrishnan. 2011. "Arginine Interactions with Anatase TiO2 (100) Surface and the Perturbation ofTi NMR Chemical Shifts-A DFTinvestigation: Relevance to Renu-Seeram Bio Solar Cell." *Journal of Molecular Modeling* 17: 1467–72.

Kulhánek, J, and F Bureš. 2012. "Imidazole as a Parent π-conjugated Backbone in Charge-Transfer Chromophores. Beilstein." *Journal Organic Chemical* 8: 25–49.

Manzhos, Sergei, Giacomo Giorgi, and Koichi Yamashita. 2015. "A Density Functional Tight Binding Study of Acetic Acid Adsorption on Crystalline and Amorphous Surfaces of Titania." *Molecules* 20: 3371–88.

Martsinovich, Natalia, and Alessandro Troisi. 2011. "Theoretical Studies of Dye-Sensitised Solar Cells: From Electronic Structure to Elementary Processes." *Energy Environment Sciences* 4: 4473–95.

Monishka, Rita Narayan. 2012. "Review: Dye Sensitized Solar Cells Based on Natural Photosensitizers." *Renewable and Sustainable Energy Reviews* 16: 208–15.

O'Regan, Brian, and Michael Gratzel. 1991. "A Low-Cost, High-Efficiency Solar Cell Based on Dye-Sintetized Colloidal TiO2 Films." *Nature* 353: 737–40.

Preat, J., C. Michaux, D Jacquemin, and E. A. Perpète. 2009. "Enhanced Efficiency of Organic Dye-Sensitized Solar Cells: Triphenylamine Derivatives." *Journal Physical Chemical C* 113: 16821–33.

Quartarolo, Angelo Domenico, and Nino Russo. 2011. "A Computational Study (TDDFT and RICC2) of the Electronic Spectra of Pyranoanthocyanins in the Gas Phase and Solution." *Journal Chemical Theory Computation* 7: 1073–81.

Sánchez De Armas, Rocío, Jaime Oviedo López, San Miguel, and A Miguel. 2010. "Real-Time TD-DFT Simulations in Dye Sensitized Solar Cells: The Electronic Absorption Spectrum of Alizarin Supported on TiO2 Nanoclusters." *Journal Chemical Theory Computation* 6: 2856–65.

Schmidt, M W, K K Baldridge, and A Boatz. 1993. "GAMESS." *Journal of Computational Chemistry* 14: 1347.

Soto-Rojo, Rody, Jesús Baldenebro-López, Norma Flores-Holguín, and Daniel Glossman-Mitnik. 2014. "Comparison of Several Protocols for the Computational Prediction of the Maximum Absorption Wavelength of Chrysanthemin." *Journal of Molecular Modeling* 20: 2378.

Srinivas, Kola, Chitumalla Ramesh Kumar, Manda Ananth Reddy, Kotamarthi Bhanuprakash, Vaidya Jayathirtha Rao, and Lingamallu Giribabu. 2011. "A-D Organic Dyes with Carbazole as Donor for Dye-Sensitized Solar Cells." *Synthetic Metals* 161: 96–105.

Suhaimi, Suriati, Mukhzeer Mohamad Shahimin, Ili Salwani Mohamad, and Mohd Natashah Norizan. 2013. "Comparative Study of Natural Anthocyanins Compound as Photovoltaic Sensitizer." *Advances in Environmental Biology* 7: 3617–20.

Vittadini, Andrea, Maurizio Casarin, and Annabella Selloni. 2007. "Chemistry of and on TiO2-anatase Surfaces by DFT Calculations: A Partial Review." *Theoretical Chemistry Accounts* 117: 663–71.

Xie, Mo, Fu-Quan Bai, Jian Wang, Chui-Peng Kong, Jie Chen, and Hong-Xing Zhang. 2016. "Theoretical Description of Dye Regeneration on the TiO2–Dye–Electrolyte Model." *Computational Materials Science* 111: 239–46.

Zhang, G, H Bala, Y Cheng, D Shi, X Lv, Q Yu, and P Wang. 2009. "High Efficiency and Stable Dye-Sensitized Solar Cells with an Organic Chromophore Featuring a Binary π -Conjugated Spacer." *Chemical Communicable* 28 (16): 2198–200.

Zhang, Ji. 2013. "Cyano or O-Nitrophenyl? Which Is the Optimal Electron-Withdrawing Group for the Acrylic Acid Acceptor of D-π-A Sensitizers in DSSCs? A Density Functional Evaluation." *Journal of Molecular Modeling* 19: 1597–604. y otros, y otros.

Zhang, Ji, Yu-He Kan, Li Hai-Bin, Yun Geng, Wu Yong, and Su Zhong-Min. 2012. "How to Design Proper P -Spacer Order of the DA Dyes for DSSCs? A Density Functional Response." *Dyes and Pigments* 95: 313–21.

Zhu, Chun, Jinxia Liang, and Zexing Cao. 2013. "Unique Metal Dicorrole Dyes with Excellent Photoelectronic Properties for Solar Cells: Insight from Density Functional Calculations." *Journal Physical Chemical C* 117: 13388–95.